

# Effect of Light Elements to Heterogeneity of Attenuation in the Earth's Inner Core

\*Chao Liu<sup>1</sup>, Takashi Yoshino<sup>1</sup>

1. Institute For Planetary Materials, Okayama University

Seismic observations have provided strong evidence of hemisphere variations, showing less attenuation, and lower seismic P-wave velocity in the western hemisphere than in the eastern hemisphere in the uppermost 100 km of the inner core (Deuss, 2014; Poupinet, Pillet, & Souriau, 1983; Souriau, 2015; Tanaka & Hamaguchi, 1997). Two major hypotheses have been proposed to explain these features: (a) inner core translation, wherein eastern hemisphere is melting at the surface of the inner core and the other side is solidifying (Monnereau, Calvet, Margerin, & Souriau, 2010), partial melting may play a key role to produce such attenuation heterogeneity at the inner core boundary; (b) thermochemical convection occurs (Alboussière et al., 2010; Deuss, 2014), which may cause the distribution of light elements. Therefore, knowledge of alloy with partial molten texture and anelastic behavior of light elements-bearing alloy is necessary to constrain the heterogeneity in the Earth's inner core. As sulfur and silicon have been considered to be more probable candidates of light elements in the inner core (Miller, 2009; Poirier, 1994; Sakamaki et al., 2016; Tsuchiya & Fujibuchi, 2009), we investigated the attenuation behavior of iron alloy containing these elements.

Three different alloys (iron, S-bearing, Si-bearing alloy) were studied. Starting materials, for S- and Si-bearing alloys were synthesized at 1 GPa in a piston cylinder apparatus. The S-bearing alloy was used to investigate anelastic behavior of the partial molten state. The measurement of seismic attenuation was conducted by in situ X-ray radiographic observation at 1.6 GPa and up to 1473 K using the deformation-DIA press at the bending magnet beam line BL04B1 at SPring-8 (Yoshino et al., 2016). The alumina aggregate, sapphire single crystal and forsterite single crystal were used as a reference material in a series of experiments. The periods of oscillation were from 0.5 to 100 s.

Pure iron with average grain size, 10  $\mu\text{m}$ , showed no frequency dependence of seismic attenuation factor  $Q^{-1}$  in bcc phase, and weak temperature dependence. For S-bearing samples with initially partial molten texture, melt separation occurred during experiment. The attenuation information of partial molten state could not be obtained. Attenuation of Si-bearing samples (average grain size larger than 1 mm) became larger with increasing Si-concentration, and showed no frequency and temperature dependences.

The experimental results showed that the seismic attenuation of Fe alloy is not frequency (0.01-2 Hz) dependent, which is consistent with the observed seismic data that there is no frequency dependence in some range of frequency due to different relaxation time in the uppermost inner core (Li & Cormier, 2002; Souriau & Roudil, 1995). The silicon can influence the heterogeneity of attenuation in the Earth's inner core. If silicon is one of the dominant light elements in the core, which means the concentration of silicon in west hemisphere is higher than it in east hemisphere in the uppermost 100 km of the inner core combined with the sound velocity data of Si-bearing alloy (Lin, 2003). So it can support the opinion that the core freezes in western hemisphere in uppermost of the inner core, growing the solid inner core and releasing silicon (Gubbins et al., 2011; Monnereau et al., 2010). It is needed to constrain the relationship between seismic attenuation and molten state.

Keywords: heterogeneity, inner core, attenuation, light element, partial melting

## 転位が岩石の非弾性に与える影響：有機多結晶体を用いたアナログ実験 Effect of dislocation on rock anelasticity: Analogue experiment using organic polycrystals

\*佐々木 勇人<sup>1</sup>、武井 康子<sup>1</sup>、マッカーシー クリスティーン<sup>2</sup>、鈴木 彩子<sup>1</sup>

\*Yuto Sasaki<sup>1</sup>, Yasuko Takei<sup>1</sup>, Christine McCarthy<sup>2</sup>, Ayako Suzuki<sup>1</sup>

1. 東京大学地震研究所、2. コロンビア大学ラumont・ドアティ地質研究所

1. Earthquake Research Institute, University of Tokyo, 2. Lamont-Doherty Earth Observatory, Columbia University

地震波速度と減衰という2つの観測量は岩石の弾性と非弾性を反映した情報であるため、これらの観測から地球内部の状態を推定するには弾性と非弾性のふるまいを理解する必要がある。岩石の非弾性メカニズムは詳しくは明らかにされていないが、粒界すべりと転位運動の主に2つが提案されている。粒界は面欠陥として、転位は線欠陥として岩石中に普遍的に存在し、地震波伝播の際にすべり運動することでエネルギーを散逸させて、地震波の速度分散と減衰を引き起こす。実験の難しさから、転位による岩石非弾性の実験的研究は粒界すべりに比べて限られており [1, 2]、詳細なメカニズムを明らかにするにはデータが不足している。そこで本研究では、岩石アナログ物質を使用した常温常圧実験によって、転位が引き起こす非弾性の高精度、広周波数帯域での測定を実現する。

岩石アナログ物質には、ボルネオール多結晶 [3] を用いた。この物質では、粒界による非弾性がすでに詳細に調べられているため [4, 5, 6]、そこからのずれとして転位の影響を調べることができる。まず、この試料に転位を導入するための温度・差応力条件を調べるため、変形機構図（差応力  $\sigma$  と歪速度  $d\varepsilon/dt$  の関係）の作成を行った。封圧 0.8 MPa、温度 40°C、50°C において、様々な1軸圧縮応力下で変形し、流動則を求めた。その結果、50°C で差応力が 1 MPa を上回ると、拡散クリープから転位クリープ ( $d\varepsilon/dt \propto \sigma^5$ ) に遷移することが分かった。転位クリープが生じたことは微細構造中の粒界移動の痕跡からも裏付けられた。

次に、決定した条件下で転位クリープさせた試料の非弾性を、 $10^{-4}$ – $10^2$  Hz の帯域における強制振動実験 [5] によって測定した。拡散クリープ領域 ( $\sigma = 0.27$  MPa)、遷移領域 ( $\sigma = 1.3$  MPa)、転位クリープ領域 ( $\sigma = 1.9$  MPa) の3つの差応力条件を選び、小さい差応力条件から大きい条件へと順に変えて1つの試料を変形させ、各変形後の非弾性特性を測定した。非弾性測定では、1軸応力の正弦的な変化に対する1軸歪応答を測定する強制振動実験を行い、ヤング率と減衰（非弾性特性）を求めた。その結果、高差応力下でのクリープ後ほどヤング率が減少し、減衰が増加した。更に、こうした非弾性特性の変化は、10日～2週間程度かけて行った非弾性測定の間、拡散クリープ後の状態までほぼ完全に回復することも分かった。これらの結果から、転位クリープによって試料中に導入された転位によって非弾性が増大し、その転位が回復（消滅）することで非弾性特性も回復したと解釈される。

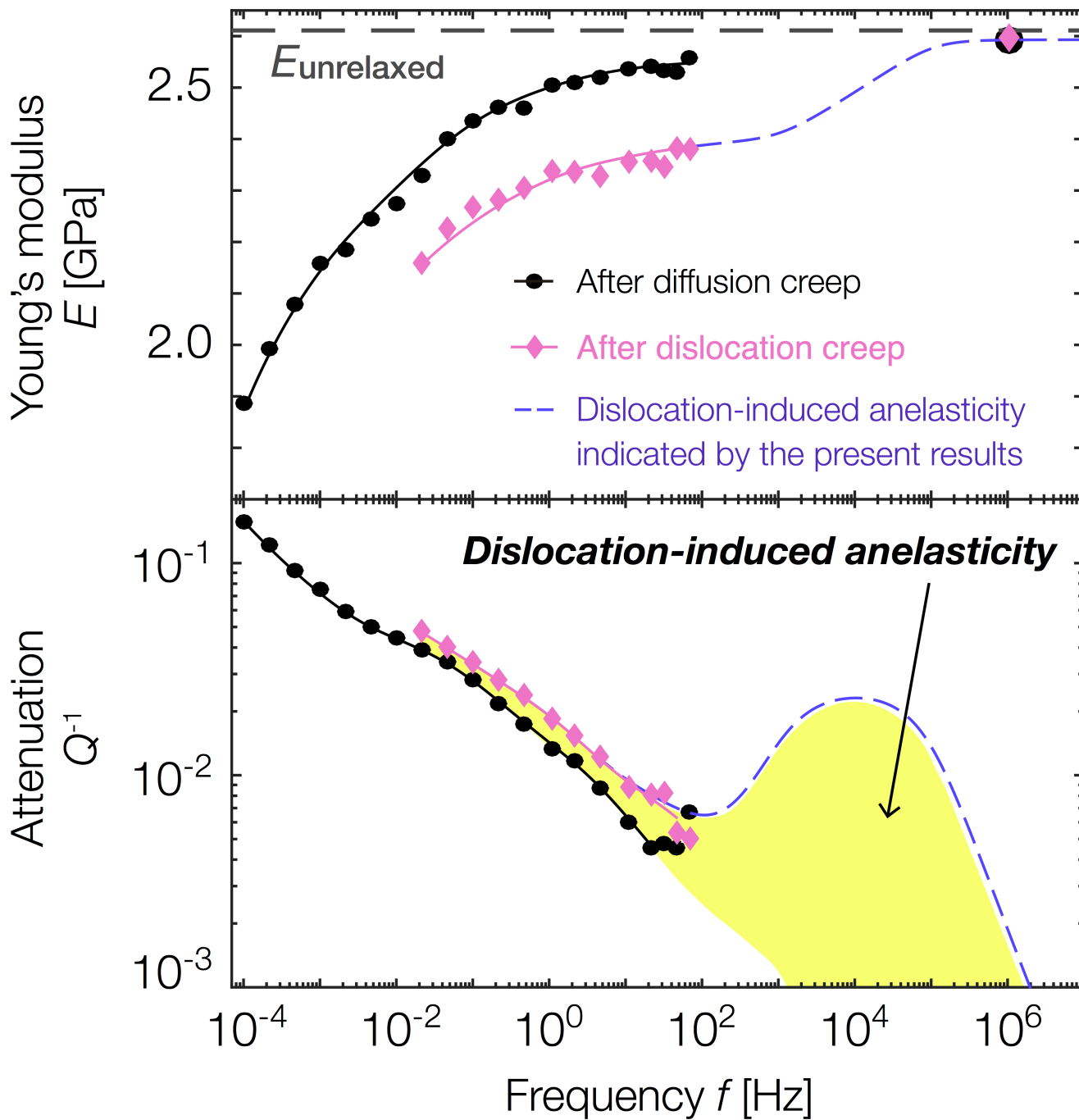
更に、転位による非弾性緩和の時間スケールを制約するための実験を行った。転位クリープ領域 ( $\sigma = 1.9$  MPa) の差応力条件下で変形させた別試料のヤング率を、変形前後において、中心周波数が  $10^6$  Hz の超音波を用いて測定した。具体的には、試料中に超音波を伝播させて縦波と横波の速度を測定することでヤング率を求めた。その結果、 $10^6$  Hz では変形前後でヤング率が変化せず、どちらも非緩和ヤング率に一致することが分かった。

以上の結果から、本研究の多結晶体試料では、転位が引き起こす非弾性緩和の大部分は  $10^2$ – $10^6$  Hz の帯域に存在していることが明らかとなった。転位による非弾性緩和は10%程度のヤング率の低下をもたらす強度を持ち、その時間スケールは粒界によるもの比べて短かった。

- [1] Guéguen *et al.* (1989),  $Q^{-1}$  of forsterite single crystals, *Phys. Earth Planet. Inter.*
- [2] Farla *et al.* (2012), Dislocation damping and anisotropic seismic wave attenuation in Earth's upper mantle, *Science*.
- [3] Takei (2000), Acoustic properties of partially molten media studied on a simple binary system with a controllable dihedral angle, *J. Geophys. Res.*
- [4] McCarthy *et al.* (2011), Experimental study of attenuation and dispersion over a broad frequency range: 2. The universal scaling of polycrystalline materials, *J. Geophys. Res. Solid Earth*.
- [5] Takei *et al.* (2014), Temperature, grain size, and chemical controls on polycrystal anelasticity over a broad frequency range extending into the seismic range, *J. Geophys. Res. Solid Earth*.
- [6] Yamauchi and Takei (2016), Polycrystal anelasticity at near-solidus temperatures, *J. Geophys. Res. Solid Earth*.

キーワード：非弾性、転位、地震波減衰、アナログ実験、欠陥、多結晶体

Keywords: anelasticity, dislocation, seismic attenuation, analog experiment, defect, polycrystal



## 地震波エンベロープで制約された海洋リソスフェア・アセノスフェアの内部減衰

### Intrinsic Attenuations in the Oceanic Lithosphere and Asthenosphere Constrained by Seismogram Envelopes

\*竹内 希<sup>1</sup>、NOMan Project Team

\*Nozomu Takeuchi<sup>1</sup>, NOMan Project Team

1. 東京大学地震研究所

1. Earthquake Research Institute, University of Tokyo

It is widely accepted that the oceanic lithosphere and asthenosphere have high-Q and low-Q, respectively, however, it is not very clear to which extent such attenuations are affected by seismic wave scattering (e.g., Shito et al. 2015, JGR; Kennett and Furumura 2013, GJI). To distinguish the intrinsic and scattering attenuations, analyzing seismogram envelopes is known to be effective. We deployed broadband ocean bottom seismometers on the old Pacific seafloor between 2010-2014 (NOMan Project, <http://www.eri.u-tokyo.ac.jp/yesman/>). We had quite large number of aftershocks of 2011 Great Tohoku Earthquake and succeeded in obtaining envelopes of Po/So and T-phase at various distances. The data purely sample the old ocean, which should provide unique opportunities to quantitatively constrain the attenuations in the ocean. We applied our envelope simulation method (Takeuchi 2016, JGR) and obtained the attenuation model by grid-searching the best structural parameters to explain the observations.

One of the most unique features of Po/So is that spatial attenuation (i.e., energy loss rate per unit propagating distance) is independent from wave type (P- or S-wave) and frequency (Butler 1987, JGR). Several previous studies (e.g, Sereno & Orcutt 1987, JGR; Mallick & Frazer 1990, GJI) explained such features by slightly ad-hoc attenuation models (strong frequency dependency; larger P attenuations than S). In contrast, we tried to explain the observations without such assumptions and succeeded in explaining most of the observed features. The results suggest that the saturation of backscattering coefficients at higher wavenumbers is primarily responsible for the constant spatial attenuation.

キーワード：減衰、散乱波

Keywords: attenuation, scattered wave

## Seismic attenuation structure beneath Nazca Plate subduction zone in S. Peru

\*Hyoihn Jang<sup>1</sup>, Younghee Kim<sup>1</sup>, Robert Clayton<sup>2</sup>

1. School of Earth and Environmental Sciences, Seoul National University, 2. Division of Geological and Planetary Sciences, California Institute of Technology

We estimate seismic attenuation in terms of quality factors, QP and QS using P and S phases, respectively, recorded from Peru Subduction Experiment (PeruSE) array deployed above Nazca Plate subduction zone between 13°S and 18°S latitude in S. Peru. We first relocate 285 earthquakes with magnitude ranges of 4.0–6.0 and depth ranges of 20–250 km. We then assume a double-corner frequency source model to measure  $t^*$ , which is an integrated attenuation through the seismic raypath between the regional earthquakes and stations. The measured  $t^*$  are inverted to construct three-dimensional attenuation structures of S. Peru. Checkerboard test results for both QP and QS structures show that we have good resolution in the slab-dip transition zone between flat and normal slab subduction down to a depth of 120 km. Both QP and QS results show high attenuation in the mantle wedge along the normal slab-dip region. Also, both show relatively higher attenuation continued down to a depth of 100 km beneath volcanic arc and also beneath the Quimsachata volcano, located farther away from the arc. We plan to compare our results with velocity models previously derived from various tomography studies for understanding structural heterogeneity, thermal conditions, and fluid content in the study area. Also, we relate measured attenuation in the mantle wedge to material properties such as viscosity to understand the subduction zone dynamics.

Keywords: attenuation, Peru

## 紀伊半島下の詳細な地震波減衰構造

### Detailed seismic attenuation structure beneath Kii peninsula, southwestern Japan

\*北 佐枝子<sup>1</sup>、澁谷 拓郎<sup>2</sup>

\*Saeko Kita<sup>1</sup>, Takuo Shibutani<sup>2</sup>

1. 広島大学大学院理学研究科地球惑星システム学専攻、2. 京都大学防災研究所

1. Department of Earth and Planetary Systems Science, Hiroshima University, 2. Disaster Prevention Research Institute, Kyoto University

Three-dimensional seismic attenuation structure (frequency-independent  $Q_p$ ) beneath Kinki region is estimated using  $t^*$  determined by applying the S-coda wave spectral ratio method to waveform data from the nationwide dense seismic network and temporary seismic observations beneath Kinki region [Shibutani and Hirahara, 2016]. Method and analysis procedure used in Kita and Matsubara [2016] were adopted in this study. The temporary seismic observation was performed from May 2004 to March 2013. The seismic attenuation structure was imaged beneath Kii peninsula at depths down to 50 km. The resolution of the image was improved comparing to that in the previous study [Kita and Matsubara, 2016 JGR], in which only data from the nationwide dense seismic network was used. Very low- $Q_p$  portion is clearly imaged in the continental plate at depths  $\sim 30$  km beneath from Osaka to southern Kyoto. The location of the very low- $Q_p$  portion corresponds to the location of Low  $V_p$  and  $V_s$  portion by Shibutani and Hirahara [2016]. Beneath Kii peninsula, hypocenters of low frequency earthquakes determined by Ohta and Ide [2011] are located above relatively low- $Q_p$  portion within the subducting oceanic crust. The location of the relatively low- $Q_p$  beneath the low frequency earthquakes also corresponds to low  $V_p$  and low  $V_s$  portion obtained by Shibutani and Hirahara [2016]. At the depths of 30 and 50 km, high- $Q_p$  portions are imaged beneath Kumano, Shingu, Kouyasan and Izumi-Ohtsu region. The strike of the high- $Q_p$  region corresponds almost to that of segmentation boundary of  $V_p/V_s$  structure [Akuhara et al., 2013] and tremors.

キーワード：地震波減衰構造、スロー地震、地震波速度構造、 $t^*$ 、西南日本

Keywords: Seismic attenuation structure, Slow earthquakes, Seismic velocities structures,  $t^*$ , Southwestern Japan



# Seismic Attenuation Tomography of Gofar Transform Fault, East Pacific Rise Using OBS Observations

\*Haijiang Zhang<sup>1</sup>, Jing Hu<sup>1</sup>, Hao Guo<sup>1</sup>

1. University of Science and Technology of China, School of Earth and Space Sciences

Gofar transform fault of East Pacific Rise generates  $M_w$  5.5-6 large earthquakes quasi-periodically on some segments of the fault, which are separated by stationary rupture barriers. Earthquakes in the seismic cycle of the large earthquake have clear spatial and temporal evolutions. To better understand the relationship between the earthquake behavior and the physical properties of the fault zone along the strike, Woods Hole Oceanographic Institution deployed a broadband ocean bottom seismograph (OBS) array on Gofar transform fault for 1-year continuous measurements, which successfully captured a  $M_w$  6.0 earthquake on 18 September 2008 and provided an unprecedented dataset. By using  $t^*$  values determined from fitting seismic waveform frequency spectrum, we have conducted three-dimensional seismic attenuation tomography to determine along-strike attenuation structure. Combined with the high-resolution earthquake locations and  $V_p$ ,  $V_s$  and  $V_p/V_s$  models determined from seismic velocity tomography, we found that the seismicity behavior is mainly controlled by structure heterogeneities along the fault.

Keywords: Gofar transform fault, Seismic attenuation tomography, Structure segmentation